Advanced Model of Squirrel Cage Induction Machine for Broken Rotor Bars Fault Using Multi Indicators

Ilias OUACHTOUK[1], *Soumia EL HANI*[1], *Said GUEDIRA*[2], *Khalid DAHI*[1], *Lahbib SADIKI*[1]

[1]Electrical Laboratory Researche, Ecole Normale Superieure de Enseignement Technique, Mohammed V University, Avenue des Nations Unies, Agdal, Rabat, Morocco
[2]Higher National School of Mines, Ecole Nationale Superieure des Mines de Rabat, Avenue Hadj Ahmed Cherkaoui, Agdal, Rabat, Morocco

ilias_ouachtouk@um5.ac.ma, s.elhani@um5s.net.ma, guedira@enim.ma, khalid.dahi@um5s.net.ma, Lahbib.sadiki@um5s.net.ma

DOI: 10.15598/aeee.v14i5.1705

Abstract. *Squirrel cage induction machine are the most commonly used electrical drives, but like any other machine, they are vulnerable to faults. Among the widespread failures of the induction machine there are rotor faults. This paper focuses on the detection of broken rotor bars fault using multi-indicator. However, diagnostics of asynchronous machine rotor faults can be accomplished by analysing the anomalies of machine local variable such as torque, magnetic flux, stator current and neutral voltage signature analysis. The aim of this research is to summarize the existing models and to develop new models of squirrel cage induction motors with consideration of the neutral voltage and to study the effect of broken rotor bars on the different electrical quantities such as the park currents, torque, stator currents and neutral voltage. The performance of the model was assessed by comparing the simulation and experimental results. The obtained results show the effectiveness of the model, and allow detection and diagnosis of these defects.*

Keywords

Diagnostic, neutral voltage signature, park currents, squirrel cage induction machine, stator current signature.

1. Introduction

The squirrel-cage induction machines are widely used and are the most common type of electrical rotating machine used in industry. However, due to the combination of poor working environment and installation, internal faults frequently occur on rotor, such as broken rotor bars, end ring connectors and eccentricities [1]. Detection of these faults is an absolute must in any real-life engineering system. Detection of broken rotor bar, particularly at an early stage, is rather difficult than stator faults [2] and [3]. This research is important because that even if though broken bars do not cause motor failures initially, they can significantly lower the efficiency and shorten the durability of induction machines.

In order to deal with the problems connected with these failures, a numerical simulation model is usually implemented to improve traditional techniques. In fact, some companies use simulation technique for designing their new product [4]. To detect the mechanical or electrical faults in induction machine, multiple methods have been utilized in the literature such as: Fast Fourier Transforms (FFT), Motor Current Signature Analysis (MCSA), Park Vectors, Stator voltages monitoring and recently Neutral Voltage (NV) [5] and [6]. Generally, MCSA is the most commonly used technique because it is simple and effective in appropriate conditions. However, this technique has significant limitations due to the increasing complexity of electrical machines and drives [10]. In order to reduce these limitations, the neutral voltage signature analysis has been used. This technique focuses on the use of voltage be-

tween the stator neutral voltage and an artificial supply neutral voltage [11] and [12].

To demonstrate the performance of the model, a comparison between simulation and experimental results have been verified, the obtained results show the effectiveness of the model, and allow detection and diagnosis of broken rotor bars defects.

2. Detection of Broken Rotor Bars

Among the widespread failures of the induction machine are the rotor faults, precisely broken rotor bars, end ring connectors and eccentricities. Rotor faults lead to speed fluctuation, torque pulsation, changes of the frequency component in the supplying neutral voltage and current of the motor, temperature increase, arcing in the rotor, and vibration of the machine. These side effects have been utilized in recent years for detecting and diagnosing this type of fault [13] and [14].

2.1. Line Current Spectrum Analysis

Motor Current Signature Analysis (MCSA), based on spectrum amplitude, have been widely used to detect broken rotor bars and end ring faults. This technique analyses the anomaly, which corresponds to broken bar faults in motor stator current spectrum, and then predicts the existence of the faults. Considering the speed ripple effect, it was reported that other frequency components of stator current due to rotor asymmetry could be observed around the fundamental at the following frequencies [8]:

$$f_b = (1 \pm 2 \cdot k \cdot s)\, f_s, \tag{1}$$

where s is slip, f_s is supply frequency and $k = 1, 2, 3, \ldots$

Other higher harmonic components can be also induced nearby to the rotor slot harmonics in the stator current spectrum:

$$f_{hk} = f_s \left[\lambda \frac{N_r}{p} (1 - s) \pm 1 \pm 2 \cdot k \cdot s \right], \tag{2}$$

where s is slip, f_s is supply frequency, λ is positive integer, N_r is number of rotor bars, p is number of pole pairs and $k = 1, 2, 3, \ldots$

2.2. Line Neutral Voltage Spectrum Analysis

The proposed approach based on spectral analysis of line-neutral voltage focuses on the use of voltage between the supply and the stator neutrals for broken rotor bars detection. Broken rotor bars causes asymmetries in the mutual inductance of the machine, which gives rise to reveal of additional components in the spectrum of the neutral voltage at frequencies given by the relation:

$$f_h = f_s \left[3h - (3h \pm 1)\, s \right], \tag{3}$$

where s is slip, f_s is supply frequency and $h = 1, 3, 5, \ldots$

The speed ripple induced additional harmonic components around the previous frequency given by Eq. (3), and frequencies of all components can be expressed as follows:

$$f_h = f_s \left[3h \cdot (1 - s) \pm s\,(1 + 2k) \right], \tag{4}$$

where s is slip, f_s is supply frequency, $k = 1, 2, 3, \ldots$ and $h = 1, 3, 5, \ldots$

The following Tab. 1 presents a summary of frequency components of motor current signature analysis and neutral voltage signature analysis.

3. Squirrel Cage Induction Motor Model

The model is built considering that both stator and rotor consist of multiple inductive circuits coupled together, and the current in each circuit is considered as an independent variable. We include in this model the most important supply voltage harmonics but also a large number of space harmonics. These harmonic spaces allow obtaining a machine model closer to the real one. However, the main information for the detection of broken bars is at the level of harmonic 3 in this voltage. The model of the induction motor takes into account the following assumptions [13], [14], [16] and [18]:

- saturation is neglected,
- uniform air gap,
- neglecting inter-bar currents,
- evenly distributed rotor bars,
- neglecting flux coupling between different winding without air gap crossing.

3.1. System of Equations

The Stator comprises conventional three phase windings, thus three circuits are required to represent the stator. The rotor consists of N_r identical and equally

Tab. 1: Frequency components of broken rotor bars motor faults.

Signature analysis	Components frequency	Harmonic components frequency
Motor Current	$f_b = (1 \pm 2 \cdot k \cdot s) f_s$	$f_{hk} = f_s \left[\lambda \frac{N_r}{p} (1-s) \pm 1 \pm 2 \cdot k \cdot s\right]$
Neutral voltage	$f_h = f_s \left[3h - (3h \pm 1)\, s\right]$	$f_h = f_s \left[3h \cdot (1-s) \pm s\,(1+2k)\right]$

spaced bars shorted together by two identical end rings [13]. Voltage equations for the motor can be written in vector-matrix form as follows:

$$\begin{cases} \mathbf{V}_s = \mathbf{R}_s \cdot \mathbf{I}_s + \dfrac{d\mathbf{\Phi}_s}{dt}, \\ \mathbf{V}_r = \mathbf{R}_r \cdot \mathbf{I}_r + \dfrac{d\mathbf{\Phi}_r}{dt}, \\ \mathbf{\Phi}_s = \mathbf{L}_s \cdot \mathbf{I}_s + \mathbf{M}_{sr} \cdot \mathbf{I}_r, \\ \mathbf{\Phi}_r = \mathbf{L}_r \cdot \mathbf{I}_r + \mathbf{M}_{rs} \cdot \mathbf{I}_s, \\ C_{em} = \dfrac{1}{2} \begin{bmatrix} \mathbf{I}_s \\ \mathbf{I}_r \end{bmatrix}^T \dfrac{d}{dq} \begin{bmatrix} \mathbf{L}_s & \mathbf{M}_{sr} \\ \mathbf{M}_{sr} & \mathbf{L}_r \end{bmatrix} \begin{bmatrix} \mathbf{I}_s \\ \mathbf{I}_r \end{bmatrix}, \\ W = \dfrac{dq}{dt}, \end{cases} \tag{5}$$

where $\mathbf{M}_{sr}$ is the Mutual matrix inductances between the stator and rotor, $\mathbf{R}_s$ is the Stator resistances matrix, $\mathbf{R}_r$ is the Rotor resistances matrix, $\mathbf{V}_r$ is the Rotor voltages vector, $\mathbf{V}_s$ is the Stator voltages vector, $\mathbf{\Phi}_s$ is the Stator flux vector and $\mathbf{\Phi}_r$ is the Rotor flux vector. The matrix $\mathbf{M}_{sr}$ depends on time, which necessitates the inversion of the inductance matrix $\mathbf{L}_s$ of dimension $\mathbf{N}_r + 4$ in each calculation. To make this matrix constant, we apply the Park transformation. The use of the Park transformation bypasses allows obtaining a system of equations with constant coefficients which facilitates their resolution.

3.2. Inductances Calculation

It is obvious that the calculation of all inductances is the key to successful simulation of an induction motor. These inductances are conveniently calculated using the Winding Function Approach. According to winding function theory, the inductance between any two windings i and j in any electric machine can be computed by the following equation [7] and [17]:

$$L_{ij}(\varphi) = \mu_0 \cdot L_r \int_0^{2\pi} \frac{n_i(\varphi,\theta)\, N_j(\varphi,\theta)}{e(\varphi,\theta)} d\theta, \tag{6}$$

where $\mu_0 = 4\pi \cdot 10^{-7}$ H·m^{-1}, e is the air gap length, θ is the particular rotor angular position, r is the average radius of the air gap, L the active stack length of the motor, φ angular position along the stator inner surface, and $n_i(\theta,\varphi)$, $N_j(\theta,\varphi)$ is called the winding function of circuit, i and j represent the magnetomotive force distribution along the air gap for the unit current in winding.

3.3. Quadrature-Phase Model

The Park transformation is a well-known three-phase to two-phase transformation in machine analysis, consisting of the application of current, voltage and flux, a change of variable by involving the angle between the axis of the windings and the d and q axes. We transform the three-phase windings a, b and c in three orthogonal d, q and o windings, referred to as [13] and [17]:

- direct axis d,
- transverse axis q,
- homopolar axis o.

The mathematical model machine equations in the axis system d, q can be written in vector matrix form as follows:

$$\begin{bmatrix} \mathrm{V_{0s}} \\ \mathrm{V_{ds}} \\ \mathrm{V_{qs}} \\ \\ 0 \\ 0 \\ 0 \\ 0 \\ \vdots \\ \vdots \\ 0 \\ \cdots \\ 0 \\ \\ 0 \end{bmatrix} = \mathbf{L}_{\mathrm{tr}} \frac{\mathrm{d}}{\mathrm{dt}} \begin{bmatrix} \mathrm{I_{0s}} \\ \mathrm{I_{ds}} \\ \mathrm{I_{qs}} \\ \\ \mathrm{I_{r0}} \\ \mathrm{I_{r1}} \\ \mathrm{I_{r2}} \\ \mathrm{I_{r3}} \\ \vdots \\ \vdots \\ \mathrm{I_{rk}} \\ \cdots \\ \mathrm{I_{r(N_r-1)}} \\ \\ \mathrm{I_e} \end{bmatrix} + \mathbf{R}_{\mathrm{tr}} \begin{bmatrix} \mathrm{I_{0s}} \\ \mathrm{I_{ds}} \\ \mathrm{I_{qs}} \\ \\ \mathrm{I_{r0}} \\ \mathrm{I_{r1}} \\ \mathrm{I_{r2}} \\ \mathrm{I_{r3}} \\ \vdots \\ \vdots \\ \mathrm{I_{rk}} \\ \cdots \\ \mathrm{I_{r(N_r-1)}} \\ \\ \mathrm{I_e} \end{bmatrix}, \tag{7}$$

and the Electromagnetic torque equation of the machine is defined as follows:

$$C_e = \sqrt{\frac{3}{2}} p L_{sr} \left(I_{qs} \sum_{k=0}^{N_r-1} I_{rk} \cos(Ka) - I_{ds} \sum_{k=0}^{N_r-1} I_{rk} \sin(Ka) \right), \tag{8}$$

where V_{sd} is the Component according to the d axis voltage, V_{sq} is the Component according to the q axis voltage, I_{sq} is the Component of the rotor current along the axis d, I_{sd} is the Component of the stator current on the axis d, I_{rq} is the Rotor current component along

the axis q, I_{rd} is the Component of the stator current on the axis q, C_{em} is the Electromagnetic torque, $\mathbf{L}_{tr}$ and $\mathbf{R}_{tr}$ are global matrices inductors and resistors obtained after the transformation of Park [13].

$$\begin{aligned} L_{sr} &= \frac{4\mu_0 N_s R l}{e\pi p^2} \sin\left(\frac{a}{2}\right), \\ a &= \frac{2\pi}{N_r}, \\ K &= 0, \ldots, N_r - 1. \end{aligned} \tag{9}$$

3.4. Line-Neutral Voltage Analysis

The approach of Neutral Voltage Signature Analysis focuses on the use of voltage between the supply and the stator neutrals [9], [11], [12] and [19]. This voltage is given by the following mathematical relationship:

$$\mathbf{V}_{3s} = \mathbf{R}_s \mathbf{i}_{3s} + \frac{d}{dt}\mathbf{\Psi}_{3s} + \mathbf{V}_{nn}, \tag{10}$$

$$\mathbf{V}_{nn} = \mathbf{R}_s \mathbf{i}_{3s} + L_a \frac{dI_{3s}}{dt} + \frac{dL_a}{d\theta}\Omega I_{3s} - \mathbf{V}_{supply}, \tag{11}$$

where $\mathbf{R}_s$ represents the stator-phase resistance, L_a his inductance, I_{sa} is the current passing through it, Ω is the rotation speed, θ is the angular position of the rotor and $\mathbf{V}_{supply}$ is simple voltage generated by network supply.

In order to depict the harmonic components related to broken rotor bars defects in the line neutral voltage, it is necessary to explore its theoretical formula.

As the stator windings are star-connected then:

$$\begin{cases} v_{sa} + v_{sb} + v_{sc} = 3v_{so}, \\ i_{sa} + i_{sb} + i_{sc} = 0, \end{cases} \tag{12}$$

and

$$v_{so} = \sum_{h=1}^{\infty} V_{soh} \cos\left(h\omega_s t + \varphi_h\right), \tag{13}$$

where v_{os} is the zero-sequence component of the supply voltage.

By the summation of the Eq. (10) and Eq. (13) we get:

$$v_{nn} = -\frac{1}{3}\left(\frac{d\Psi_{sa}}{dt} + \frac{d\Psi_{sb}}{dt} + \frac{d\Psi_{sc}}{dt}\right). \tag{14}$$

The mutual inductance as described by Eq. (15) presents harmonics with respect to the electrical angle θ, where $a = p(2\pi \cdot N_r^{-1})$ is the electrical angle of a rotor loop.

Therefore, the line voltage between neutrals can be written as Eq. (16), where V_{nn} is the potential difference between the neutral of star-connected stator and the neutral network in the case of a direct feed or artificial neutral in the case of a supply voltage by inverter results in healthy condition of induction motor.

4. Simulation Results Analysis

For a squirrel cage induction motor with N_r bars, and one end ring current, Eq. (7) and Eq. (8) can be resolved using the fourth-order Runge-Kutta method. To validate the proposed model, the machine was first simulated under healthy condition. Then, the rotor faults under different broken rotor bars were simulated. The rotor has been presented by all the meshes allowing the representation of various faults, to simulate a broken rotor bar, the resistance of a bar of the cage is increased 40 times its healthy value ($R_{bb} = 40 \cdot R_b$) in the $\mathbf{R}_{tr}$ until the current in the bar is closest to zero.

4.1. Simulation and Analysis of Healthy State

The simulation study was at: no load for 1 sec and then the motor is loaded with 15 Nm load using a machine of 3 phases, 50 Hz, 48 stator slots, 28 rotor bars and 2 poles machine. The Fig. 1(a), Fig. 1(b), Fig. 1(c),

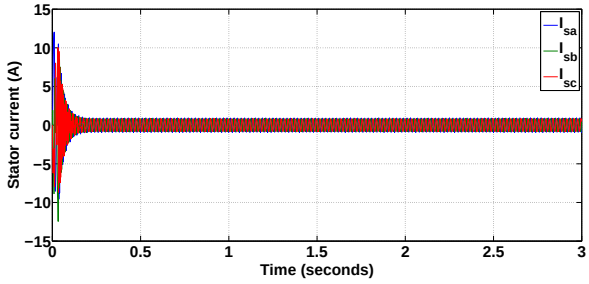

(a) Stator current at no load.

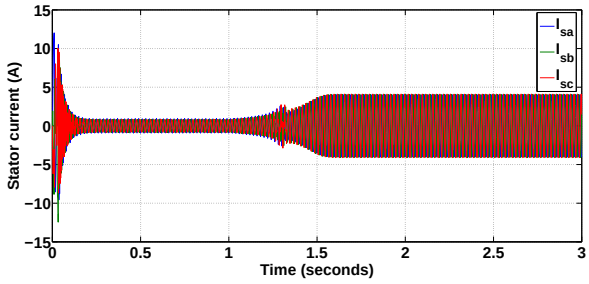

(b) Stator current when the motor is loaded.

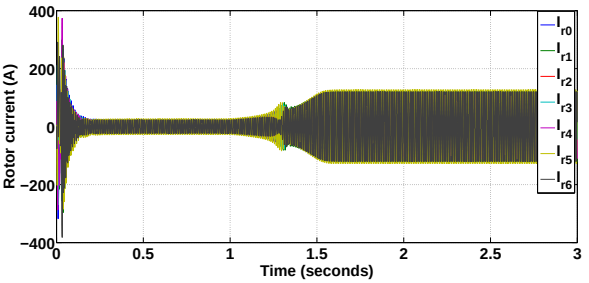

(c) Rotor currents.

$$\mathbf{M}_{sr} = \sum_{h=1}^{\infty} M_h^{sr} \cdot \begin{bmatrix} \cos(h\cdot(\theta+\phi_h)) & \dots & \cos(h\cdot(\theta+\phi_h+k\cdot a) & \dots \\ \cos(h\cdot(\theta+\phi_h-\frac{2\pi}{3})) & \dots & \cos(h\cdot(\theta+\phi_h+k\cdot a-\frac{2\pi}{3})) & \dots \\ \cos(h\cdot(\theta+\phi_h+\frac{2\pi}{3})) & \dots & \cos(h\cdot(\theta+\phi_h+k\cdot a-\frac{2\pi}{3})) & \dots \end{bmatrix}. \tag{15}$$

$$\begin{aligned} \mathbf{V}_{nn} = &-\sum_{h=1}^{\infty} M_{3h}^{sr} \left[\cos(3h(\theta+\varphi_{3h})) \quad \dots \quad \cos(3h(\theta+\varphi_{3h}+ka)) \quad \dots\right] \frac{d}{dt}\mathbf{i}_{rk} + \frac{d\theta}{dt}\sum_{h=1}^{\infty} 3hs\omega_s M_{3h}^{sr} \\ &\cdot \left[\cos(3h(\theta+\varphi_{3h})) \quad \dots \quad \cos(3h(\theta+\varphi_{3h}+ka)) \quad \dots\right] \cdot \mathbf{i}_{rk} + \sum_{h=1}^{\infty} V_{soh}\cos(h\omega_s t+\varphi_h). \end{aligned} \tag{16}$$

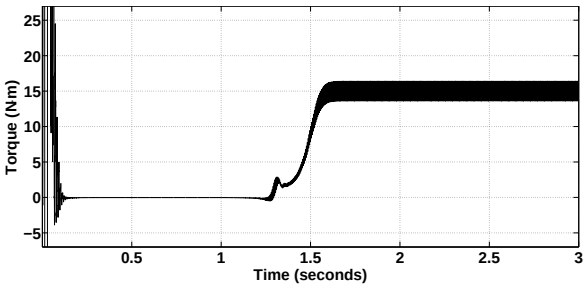

(d) Electromagnetic torque.

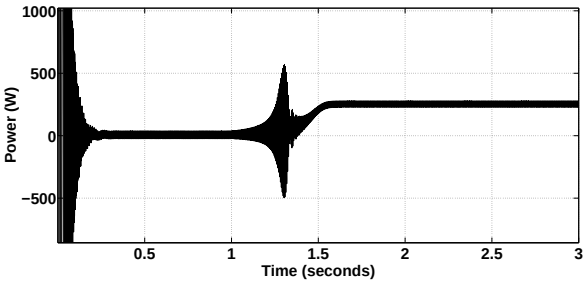

(e) Power.

Fig. 1: Simulation results of healthy state.

Fig. 1(d) and Fig. 1(e) show the simulation results in healthy condition of induction motor.

4.2. Simulation and Analysis of Broken Bars Fault in Motor

The motor is simulated at no load for 1 sec and then the motor is loaded with 15 Nm load, at 3 sec a completely broken rotor bars occur in a rotor induction motor. The Fig. 2(a), Fig. 2(b), Fig. 2(c), Fig. 2(d) and Fig. 2(e) show the simulation results for failures of the induction motor.

The impact of broken rotor bars fault on machine current can be examined through Park vector transformation approach. The current Park's vector for a healthy motor corresponds to a circle, whereas for a faulty one, the shape distorts depending upon the amount of fault level. To decide on the nature of the fault occurred in induction machine, an analysis with the well-known FFT is done to decide on the fault and also its severity. In this case, broken bars related harmonic components are clearly located around the fundamental Fig. 4.

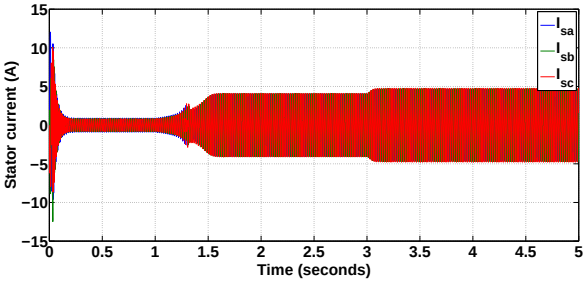

(a) Stator current.

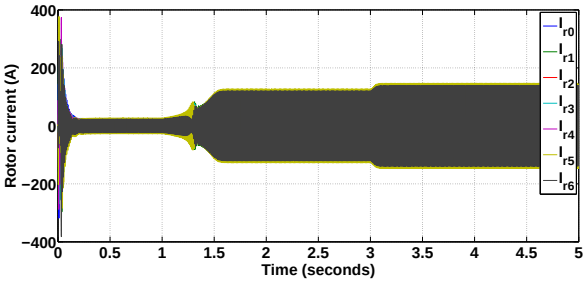

(b) Rotor currents.

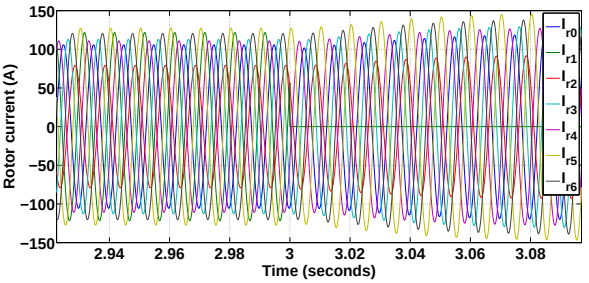

(c) Zoom of rotor currents.

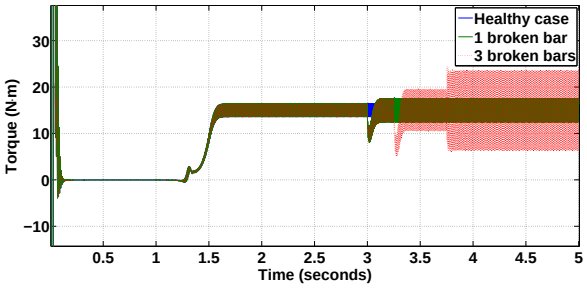

(d) Electromagnetic torque.

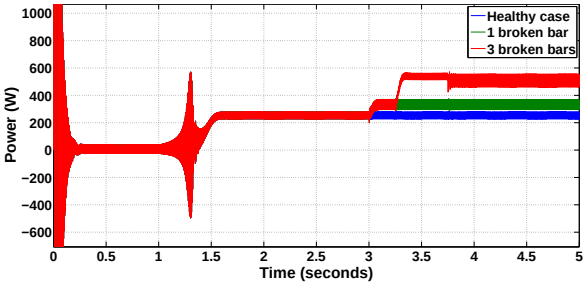

(e) Power.

Fig. 2: Simulation results of broken bars fault in motor.

5. Experimental Results Analysis

In order to test the proposed model, an experimental system is configured as shown in Fig. 6. The experimental tests were developed on a 3 kW, 50 Hz, 220 V = 380 V, 4-poles Induction Machine. The motor was directly coupled to a direct current machine acting as a load. Two voltage sensors are used to monitor the induction machine operation. The IM voltages are measured by means of the two sensors, which are used as inputs of the signal conditioning and the data acquisition board integrated into a personal computer.

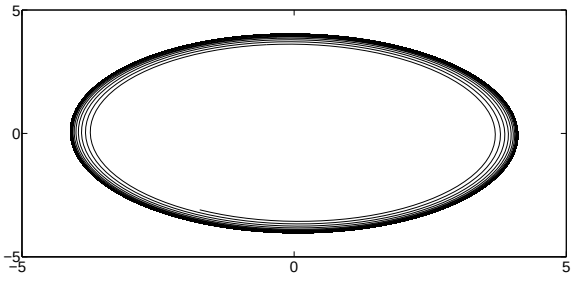

(a) Healthy case.

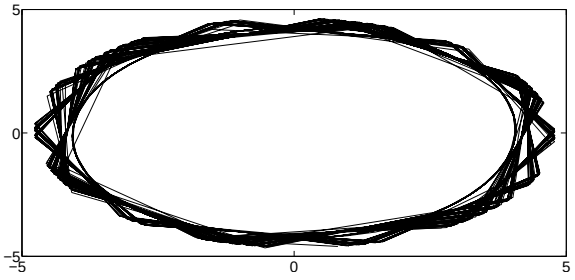

(b) Faulty case.

Fig. 3: Motor current's Park's vector representation.

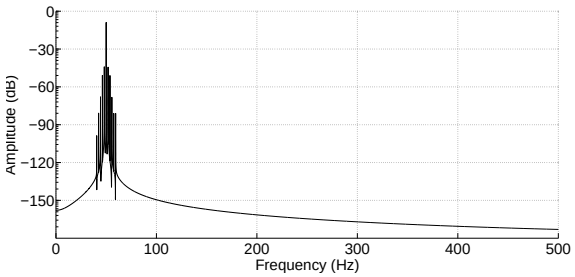

(a)

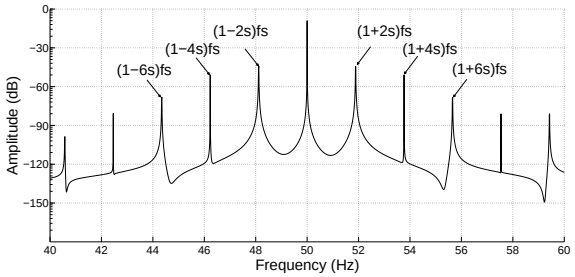

(b)

Fig. 4: Simulation: Normalized FFT spectrum of machine line current of IM with 3 broken rotor bars.

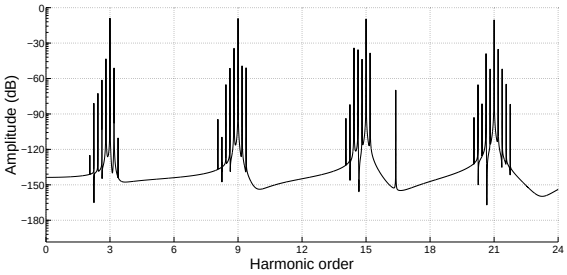

(a)

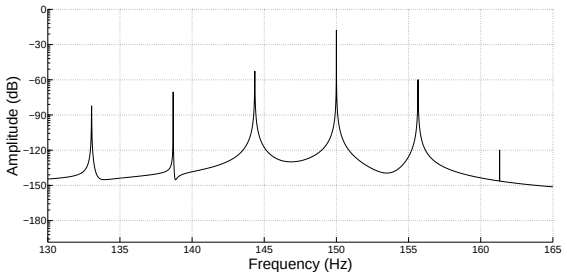

(b)

Fig. 5: (a) Simulation: Normalized FFT spectrum of machine line neutral voltage of IM with 3 broken rotor bars, (b) Zoom of line neutral voltage around the 3rd harmonic.

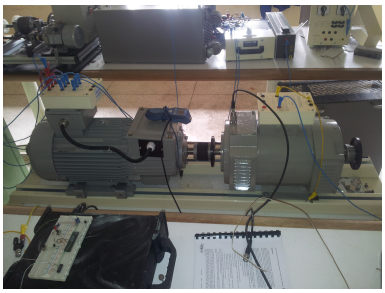

Fig. 6: Experimental setup.

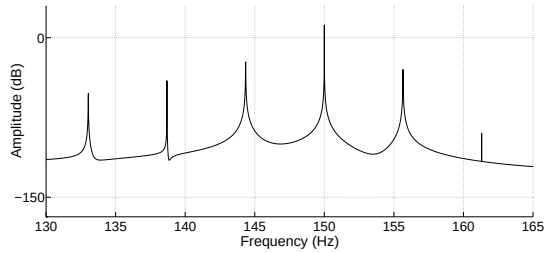

(a) Simulations results.

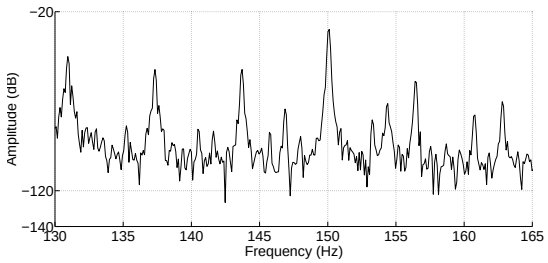

(b) Experimental results.

Fig. 7: Line neutral voltage comparison.

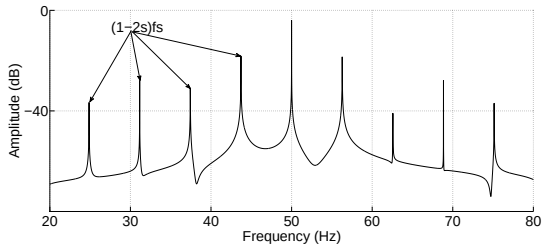

(a) Simulations results.

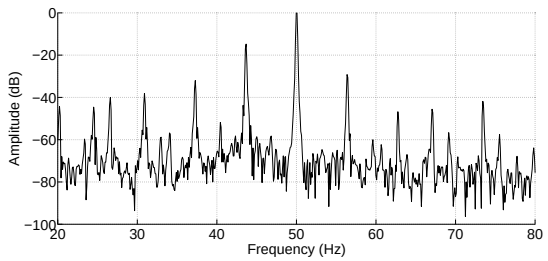

(b) Experimental results.

Fig. 8: Line current comparison.

6. Discussion

Broken rotor bars fault in induction machine lead to changes of the frequency component in the supplying neutral voltage and current of the motor, electromagnetic torque and power pulsation. The simulation results are shown in Fig. 1, Fig. 2, Fig. 3, Fig. 4, Fig. 5, Fig. 6, Fig. 7 and Fig. 8.

Figure 1 shows the simulation results of induction machine in healthy case. Figure 1(a): Stator current for no load normal condition, Fig. 1(b): Stator current when the motor is loaded, Fig. 1(c): Rotor currents, Fig. 1(d): Electromagnetic torque and Fig. 1(e): Power.

Figure 2 shows the simulation results in defect case, under one and three adjacent broken bars: Fig. 2(a): Stator current, Fig. 2(b): Rotor currents, Fig. 2(c): Zoom of rotor currents, Fig.1(d): Electromagnetic torque and Fig. 2(e): Power.

Figure 3 shows the motor current's Park's vector representation, Fig. 3(a): Healthy case, Fig. 3(b): Faulty case.

Figure 4(a) Simulation: Normalized FFT spectrum of machine line current of IM with 3 broken rotor bars and Fig. 4(b) show a zoom around the fundamental frequency.

Figure 5(a) shows the spectrum content of the line between neutrals ($\mathbf{V}_{nn}$), when a rotor dissymmetry is considered (constructional dissymmetry or broken rotor bar) under a balanced sinusoidal voltage supply. Equation (4) clarifies the frequencies of the additional harmonics, $f_h(3h, 0, \pm k)$, where $3h = 3, 9, 15, 21, 27, \ldots, \eta = 0$ and $k = 0, \pm 1, \pm 2, \pm 3, \pm 4 \ldots$. Figure 5(b) shows a zoom around the first-order harmonic $3h$, which gives $f_h(3, 0, \pm k) = 3 - (3h \pm 1)s + 2k_s$.

Figure 7 shows a Line neutral voltage comparison between the simulations results (Fig. 7(a) and experiment ones (Fig. 7(b)), we note a match between these results.

Figure 8 shows a line current comparison between the simulations results Fig. 8(a) and experiment ones Fig. 8(b), we note a match between these results. This model is helpful in quantifying the rotor slot harmonics under healthy as well as faulty condition.

7. Conclusion

In this paper, we presented a mathematical model and simulation of squirrel cage induction motor in healthy case and under defects of one and three adjacent broken bars. The particularity of the model is that it takes into account the line neutral voltage in the sys-

tem equation, and it is based on a detailed modeling of the induction motors, represented by m stator phases and N_r rotor bars, which allows detecting and localization of the completely and partially broken rotor bars with multi indicators, without the need to change the model structure. The simulation results show the effectiveness of the model as it adapts with the presented problem and it shows a good match with the theoretical predictions. The accuracy of the simulation results is verified by the experimental results.

The results presented in this paper are promising and clear and thus the future research work should focus on the use of information collected from multiple sensors (indicators), such as current, voltage, torque, vibration, and temperature, to detect and identify motor faults.

References

[1] CHEN, S. and R. ZIVANOVIC. A novel high-resolution technique for induction machine broken bar detection. In: *Australasian Universities Power Engineering Conference*. Perth: IEEE, 2007, pp. 1–5. ISBN 978-0-646-49488-3. DOI: 10.1109/AUPEC.2007.4548040.

[2] CALIS, H. and A. CAKIR. Experimental study for sensorless broken bar detection in induction motors. *Energy Conversion and Management*. 2008, vol. 49, iss. 2, pp. 869–875. ISSN 0196-8904. DOI: 10.1016/j.enconman.2007.06.030.

[3] GODOY, W. F., I. N. DA SILVA, A. GOEDTEL, R. H. C. PALACIOS and T. D. LOPES. Application of intelligent tools to detect and classify broken rotor bars in three-phase induction motors fed by an inverter. *IET Electric Power Applications*. 2016, vol. 10, iss. 5, pp. 430–439. ISSN 1751-8679. DOI: 10.1049/iet-epa.2015.0469.

[4] KAZAKOV, J. and I. PALILOV. Research Related Electromechanical Processes in an Asynchronous Traction Motor - Asynchronous Generator with Common Shaft Based on Field Model. *Advances in Electrical and Electronic Engineering*. 2010, vol. 13, no. 5, pp. 442–446. ISSN 1804-3119. DOI: 10.15598/aeee.v13i5.1388.

[5] DAHI, K., S. ELHANI and S. GUEDIRA. Wound-rotor IM diagnosis method based on neutral voltage signal analysis. In: *40th Annual Conference of the IEEE Industrial Electronics Society*. Dallas: IEEE, 2014, pp. 965–971. ISBN 978-1-4799-4032-5. DOI: 10.1109/IECON.2014.7048618.

[6] MENACER, A., M.-S. NAIT-SAID, A. BENAKCHA and S. DRID. Stator current analysis of incipient fault into asynchronous motor rotor bars using Fourier fast transform. *Journal of Electrical Engineering*. 2004, vol. 55, no. 5–6, pp. 122–130. ISSN 1335-3632.

[7] JUNG, J.-H., J.-J. LEE and B.-H. KWON. Online Diagnosis of Induction Motors Using MCSA. *IEEE Transactions on Industrial Electronics*. 2006, vol. 53, iss. 6, pp. 1842–1852. ISSN 1557-9948. DOI: 10.1109/TIE.2006.885131.

[8] GU, F., T. WANG, A. ALWODAI, X. TIAN, Y. SHAO and A. D. BALL. A new method of accurate broken rotor bar diagnosis based on modulation signal bispectrum analysis of motor current signals. *Mechanical Systems and Signal Processing*. 2015, vol. 50, iss. 1, pp. 400–413. ISSN 0888-3270. DOI: 10.1016/j.ymssp.2014.05.017.

[9] KHEZZAR, A., M. E. K. OUMAAMAR and M. HADJAMI. Induction Motor Diagnosis Using Line Neutral Voltage Signatures. *IEEE Transactions on Industrial Electronics*. 2008, vol. 56, iss. 11, pp. 4581–4591. ISSN 1557-9948. DOI: 10.1109/TIE.2008.2010209.

[10] FILIPPETTI, F., A. BELLINI and G.-A. CAPOLINO. Condition monitoring and diagnosis of rotor faults in induction machines: State of art and future perspectives. In: *1st IEEE Workshop on Electrical Machines Design, Control and Diagnosis*. Paris: IEEE, 2013, pp. 196–209. ISBN 978-1-4673-5657-2. DOI: 10.1109/WEMDCD.2013.6525180.

[11] DAHI, K., S. ELHANI, S. GUEDIRA, L. SADIKI and I. OUACHTOUK. High-resolution spectral analysis method to identify rotor faults in WRIM using Neutral Voltage. In: *1st International Conference on Electrical and Information Technologies*. Marrakech: IEEE, 2015, pp. 82–87. ISBN 978-1-4799-7479-5. DOI: 10.1109/EITech.2015.7162988.

[12] OUMAAMAR, M. E. K., A. KHEZZAR, M. BOUCHERMA, H. RAZIK, R. N. ANDRIAMALALA and L. BAGHLI. Neutral Voltage Analysis for Broken Rotor Bars Detection in Induction Motors Using Hilbert Transform Phase. In: *42nd Annual Meeting of the IEEE-Industry-Applications-Society*. New Orleans: IEEE, 2007, pp. 1940–1947. ISBN 978-1-4244-1259-4. DOI: 10.1109/07IAS.2007.295.

[13] OUACHTOUK, I., S. E. HANI, S. GUEDIRA, L. SADIKI and K. DAHI. Modeling of squirrel cage induction motor a view to detecting broken rotor bars faults. In: *1st International Conference on Electrical and Information Technologies*. Marrakech: IEEE, 2015, pp. 347–352. ISBN 978-1-4799-7479-5. DOI: 10.1109/EITech.2015.7163001.

[14] MUSTAFA, M. O., G. NIKOLAKOPOULOS and T. GUSTAFSSON. Broken bars fault diagnosis based on uncertainty bounds violation for three-phase induction motors. *International Transactions on Electrical Energy Systems*. 2013, vol. 25, iss. 2, pp. 402–409. ISSN 2050-7038. DOI: 10.1002/etep.1843.

[15] WALLACE, A. K. and A. WRIGHT. Novel Simulation of Cage Windings Based on Mesh Circuit Model. *IEEE Transactions on Power Apparatus and Systems*. 1974, vol. PAS-93, iss. 1, pp. 377–382. ISSN 0018-9510. DOI: 10.1109/TPAS.1974.293957.

[16] DELFORGE, C. and B. LEMAIRE-SEMAIL. Measuring the efficiency of decision making units. *IEEE Transactions on Magnetics*. 1995, vol. 31, iss. 3, pp. 2092–2095. ISSN 0018-9464. DOI: 10.1109/20.376457.

[17] FILIPPETTI, F., A. BELLINI and G.-A. CAPOLINO. Condition monitoring and diagnosis of rotor faults in induction machines: State of art and future perspectives. In: *1st IEEE Workshop on Electrical Machines Design, Control and Diagnosis*. Paris: IEEE, 2013, pp. 196–209. ISBN 978-1-4673-5657-2. DOI: 10.1109/WEMDCD.2013.6525180.

[18] SINGH, A., B. GRANT, R. DEFOUR, C. SHARMA and S. BAHADOORSINGH. A review of induction motor fault modeling. *Electric Power Systems Research*. 2016, vol. 133, iss. 1, pp. 191–197. ISSN 0378-7796. DOI: 10.1016/j.epsr.2015.12.017.

[19] DAHI, K., S. E. HANI, S. GUEDIRA and I. OUACHTOUK. A New Indicator for Rotor Asymmetries in Induction Machines Based on Line Neutral Voltage. *Research Journal of Applied Sciences, Engineering and Technology*. 2016, vol. 12, iss. 11, pp. 1136–1145. ISSN 2040-7467. DOI: 10.19026/rjaset.12.2855.

About Authors

Ilias OUACHTOUK was born in Foum Zguid-Tata, Morocco, in 1991. He received his M.Sc. degree in electrical engineering from the Mohammed V University in Rabat, Morocco, in 2014. Where he is currently working toward the Ph.D. degree, in the department of electrical engineering. Since 2015. His research interests include modeling and diagnosis of electrical drives, in particular, synchronous and asynchronous motors.

Soumia EL HANI has been Professor at the ENSET (Ecole Normale Superieure de l'Enseignement Technqique - Rabat, Morroco) since October 1992. She is a Research Engineer at the Mohammed V University in Rabat Morocco, in charge of the research team electromechanical, control and diagnosis, IEEE member, member of the research laboratory in electrical engineering at ENSET - Rabat. Author of several publications in the field of electrical engineering, including robust control systems, diagnosis and control systems of wind electric conversion. She has been general co-Chair the two editions of 'the International Conference on Electrical and Information Technologies', held in Marrakech, March 2015 and Tangier, May 2016 respectively.

Said GUEDIRA Professor at ENSMR (Ecole Nationale des Mines de Rabat Morroco) since 1983. Research Engineer and Director of the research laboratory CPS2I (Control, Potection et Surveillance des Installations Industrielles). Author of several publications in the field of Electrical Engineering, including diagnosis and control of mechatronic systems. His research interests are in the area of electromechanical engineering, Monitoring and Diagnosis of Mechatronic Systems.

Khalid DAHI was born in Errachidia, Morocco, in 1988. He received the M.Sc. degree in electrical engineering in 2012 from the Mohammed V University in Rabat- Morocco. Where he is currently working toward the Ph.D. degree in the department of electrical engineering. Since 2012, His research interests are related to electrical machines and drives, diagnostics of induction motors. His current activities include monitoring and diagnosis of induction machines in wind motor.

Lahbib SADIKI was born in Errachidia, Morocco, in 1987. He received the M.Sc. degree in electrical engineering in 2013 from the Mohammed V University in Rabat- Morocco. Where he is currently working toward the Ph.D. degree in the department of electrical engineering. Since 2014, His research interests are related to electrical machines and drives, diagnostics of induction motors. His current activities include monitoring and diagnosis of induction machines.

Appendix A

Tab. 2: Units for magnetic properties.

Symbol	Quantity	Numerical application
P	Power	5 kW
U	Power supply voltage	380 V
f	Current stator frequency	50 Hz
p	Number of pole pairs	2
N_r	Number of rotor bars	28
S_n	Number of stator slots	48
N_s	Number of turns in series per phase	80
e_a	Ring thickness	$0.28 \cdot 10^{-3}$ m
R_s	Resistance of a stator Phase	1.5 Ω
R_b	Resistance of a rotor bar	$96.9 \cdot 10^{-6}$ Ω
R_e	Resistance of a short circuit ring	$5 \cdot 10^{-6}$ Ω
L_b	Leakage inductance of a rotor bar	$0.28 \cdot 10^{-6}$ H
L_e	Leakage inductance of a ring of short circuit	$0.036 \cdot 10^{-6}$ H
j	Moment of inertia	0.0131 Kg·m^2
μ	Permeability	$4\pi \cdot 10^{-7} \frac{W_b}{\mathrm{A} \cdot \mathrm{m}}$